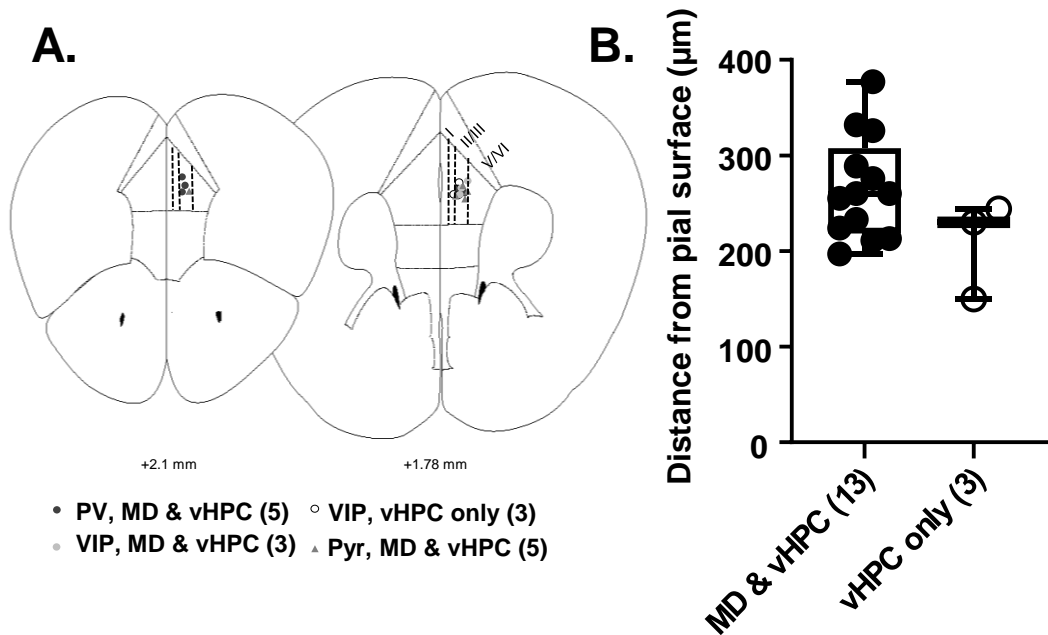
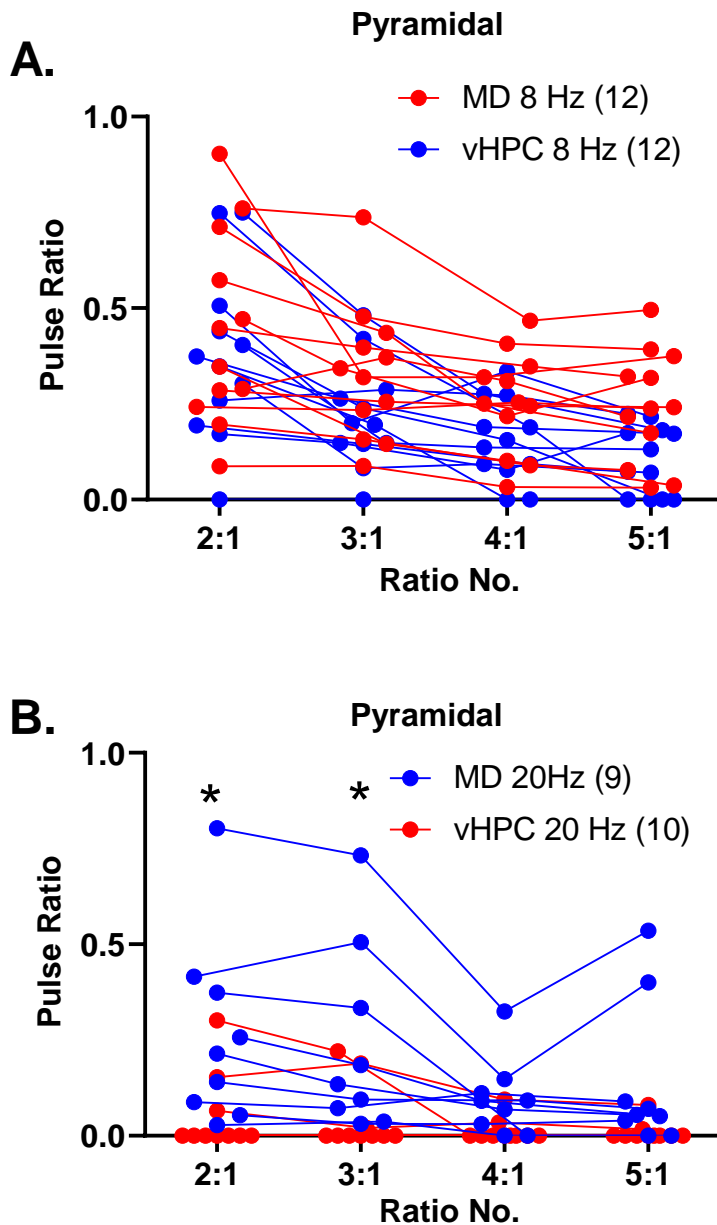


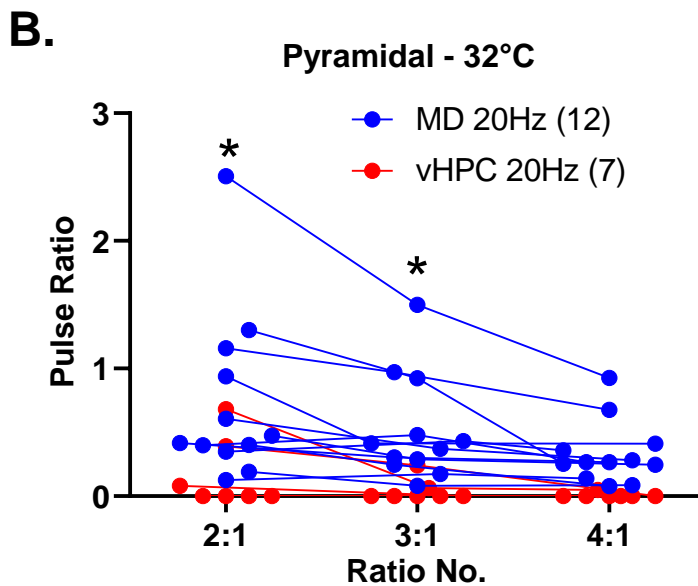
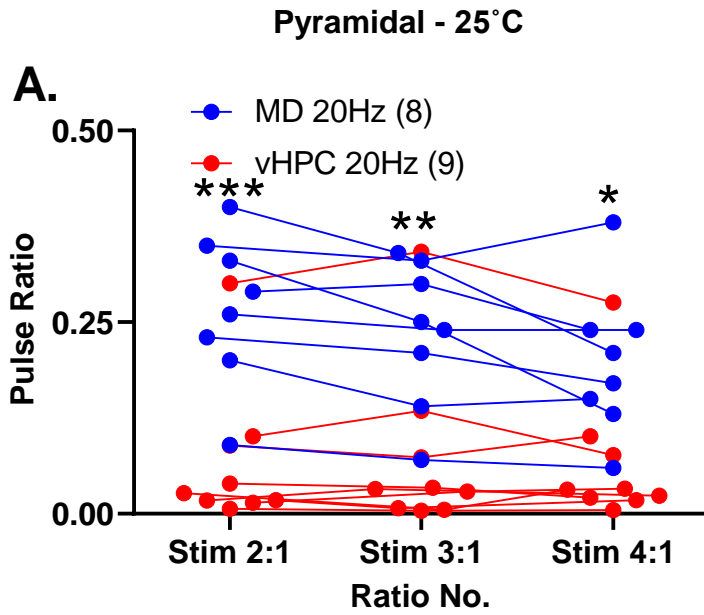
**Supplementary Figure 1. Individual data points for cells recorded in Figure 2.** (A) The amplitude of individual cell responses to repeated pulses of light at 8 Hz in response to stimulation of MD inputs expressing Chronos (green) or Chromson (red). (B) The amplitude of individual cell responses to repeated pulses of light at 20 Hz in response to stimulation of MD inputs expressing Chronos (green) or Chromson (red). (C) The ratios of individual cell responses to subsequent pulses of light relative to the first pulse in response to stimulation of MD inputs expressing Chronos (green) or Chromson (red) at 8 Hz. (D) The ratios of individual cell responses to subsequent pulses of light relative to the first pulse in response to stimulation of MD inputs expressing Chronos (green) or Chromson (red) at 20 Hz. \*\* $p < 0.01$ .



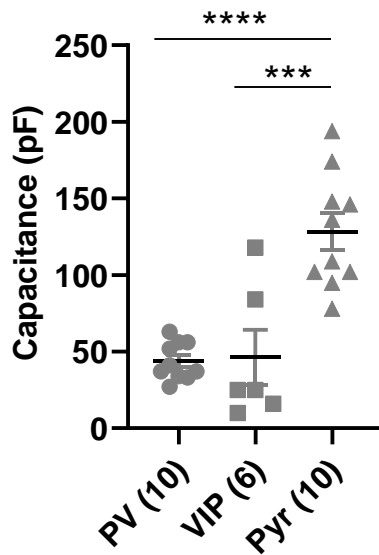
**Supplementary Figure 2. Illustration of recording location of all cells where posthoc images were collected. (A)** Images confirming the recording location were available for 5 PV, 6 VIP and 5 Pyramidal (Pyr) cells. Locations, generally clustered around the border of layer II and III, are illustrated for PV, VIP and Pyr cells that received input from both the MD and vHPC, as well as VIP cells that responded only to input the vHPC. Cell location was not available for PV cells that responded only to the MD. **(B)** The distance from the pial surface (measured in  $\mu\text{m}$ ) does not vary between these groups. One-way ANOVA, no effect of region  $F_{(2, 13)}=2.345$ ,  $p=0.135$ .



**Supplementary Figure 3. Individual data points for cells recorded in Figure 3. (A)** The ratios of individual cell responses to subsequent pulses of light relative to the first pulse in response to stimulation of MD inputs (blue) or vHPC inputs (red) at 8 Hz. **(B)** The ratios of individual cell responses to subsequent pulses of light relative to the first pulse in response to stimulation of MD inputs (blue) or vHPC inputs (red) at 20 Hz. \* $p < 0.01$ .

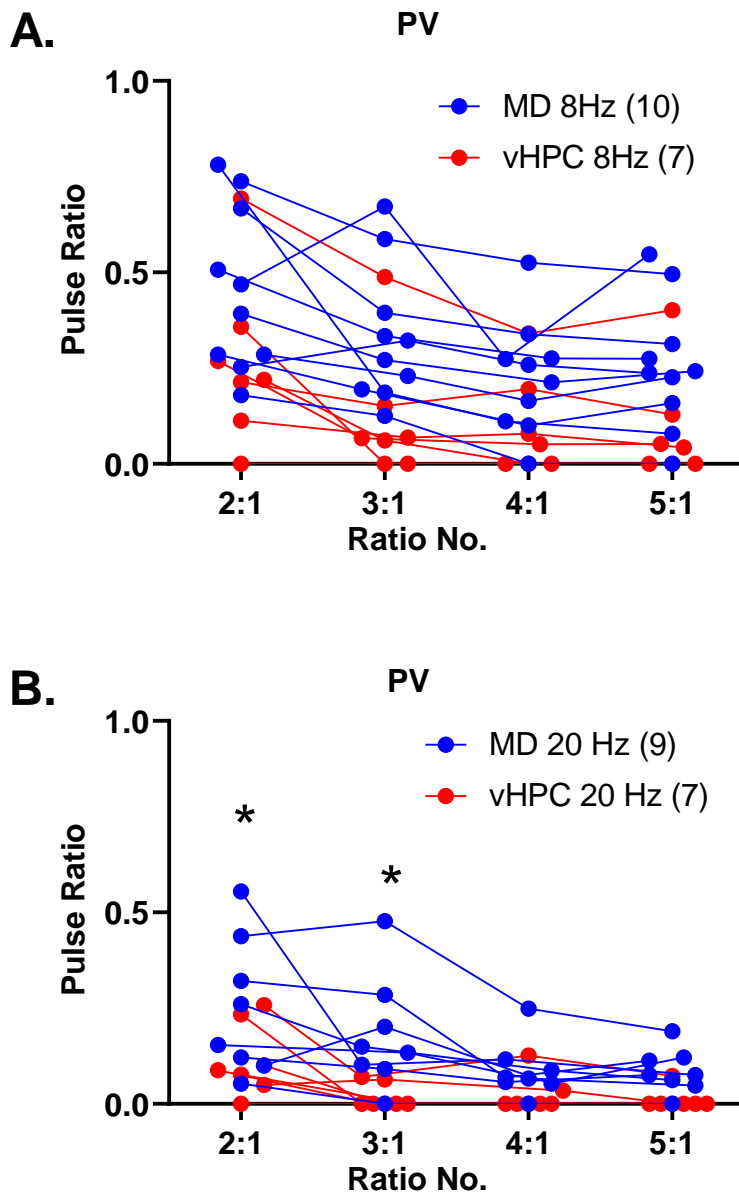


**Supplementary Figure 4. Individual data points for cells recorded in Figure 4. (A)** The ratios of individual cell responses to subsequent pulses of light relative to the first pulse in response to stimulation of MD inputs (blue) or vHPC inputs (red) at 20 Hz at 25°C. **(B)** The ratios of individual cell responses to subsequent pulses of light relative to the first pulse in response to stimulation of MD inputs (blue) or vHPC inputs (red) at 20 Hz at 32°C. \* $p < 0.05$ . \*\* $p < 0.01$ . \*\*\* $p < 0.001$ .

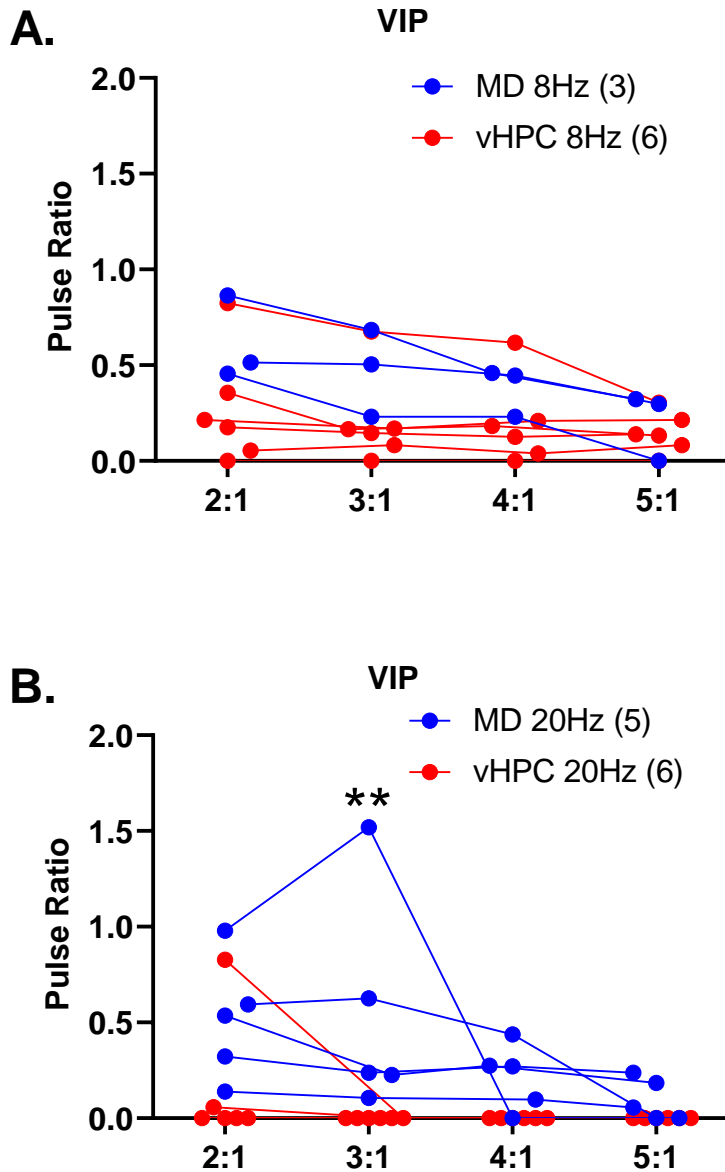


**Supplementary Figure 5. Interneuron capacitance is significantly different from that of pyramidal cells.** Capacitance measurements for PV and VIP interneurons were significantly smaller than those for Pyramidal cells (Pyr). One-way ANOVA,  $F_{(2, 23)}=21.06$ ,  $p<0.0001$ . Bonferroni post-hoc PV v Pyr, multiplicity-adjusted \*\*\*\* $p<0.0001$ ; VIP v Pyr, multiplicity-adjusted \*\*\* $p=0.0001$ .





**Supplementary Figure 7. Individual data points for cells recorded in Figure 5. (A)** The ratios of individual cell responses to subsequent pulses of light relative to the first pulse in response to stimulation of MD inputs (blue) or vHPC inputs (red) at 8 Hz. **(B)** The ratios of individual cell responses to subsequent pulses of light relative to the first pulse in response to stimulation of MD inputs (blue) or vHPC inputs (red) at 20 Hz. \* $p < 0.05$ .



**Supplementary Figure 8. Individual data points for cells recorded in Figure 6. (A)** The ratios of individual cell responses to subsequent pulses of light relative to the first pulse in response to stimulation of MD inputs (blue) or vHPC inputs (red) at 8 Hz. **(B)** The ratios of individual cell responses to subsequent pulses of light relative to the first pulse in response to stimulation of MD inputs (blue) or vHPC inputs (red) at 20 Hz. \*\* $p < 0.01$ .